

Nonlinear wave-packet dynamics for a generic one-dimensional time-independent system and its application to the hydrogen atom in a weak magnetic field

Karine Dupret and Dominique Delande

Laboratoire Kastler-Brossel, Tour 12, Etage 1, Université Pierre et Marie Curie, 4 Place Jussieu, 75005 Paris Cedex 05, France

(Received 21 July 1995; revised manuscript received 10 October 1995)

We study the time propagation of an initially localized wave packet for a generic one-dimensional time-independent system, using the “nonlinear wave-packet dynamics” [S. Tomovic and E. J. Heller, *Phys. Rev. Lett.* **67**, 664 (1991)], a semiclassical approximation using a local linearization of the wave packet in the vicinity of classical reference trajectories. Several reference trajectories are needed to describe the behavior of the full wave packet. The introduction of action-angle variables allows us to obtain a simple analytic expression for the autocorrelation function, and to show that a universal behavior (quantum collapses, quantum revivals, etc.) is obtained via interferences between the reference trajectories. A connection with the standard WKB approach is established. Finally, we apply the nonlinear wave-packet dynamics to the case of the hydrogen atom in a weak magnetic field, and show that the semiclassical expressions obtained by nonlinear wave-packet dynamics are extremely accurate.

PACS number(s): 03.65.Sq, 32.60.+i, 31.15.Gy, 31.50.+w

I. INTRODUCTION

The understanding of the transition between the classical and quantum behavior of a physical system is a very exciting challenge for the physicist. The key parameter is the ratio of the classical action along a typical short closed trajectory to the Planck constant \hbar . There are two separate ways to consider the problem. The first one, and also the more investigated so far, is to solve the time independent Schrödinger equation (for a time-independent system) in the limit of large quantum numbers, and try to express the quantized energy levels in terms of classical quantities. The second one is to study the time evolution of the closest quantum analog of a classical particle (a localized wave packet) through the time dependent Schrödinger equation, and to determine how it is linked to classical trajectories.

The simplest illustration of the first approach is the WKB method [1] for time-independent one-dimensional systems. A certain form of solution of the time-independent Schrödinger equation is assessed, in which the phase term is expanded in powers of \hbar . The boundary conditions can be satisfied only for specific values of the energy. This quantization condition has a simple physical interpretation: the energy levels correspond to classical trajectories where the action is a half-integer multiple of the Planck constant. This method can be extended to multidimensional integrable systems (it is then called the EBK method [1]), when the number of classical constants of motion is equal to the number of degrees of freedom. It can further be used for quasi-integrable systems (the so-called “torus quantization”) when the classical motion, although not strictly integrable, is mainly regular, but it cannot be used for chaotic or mixed regular-chaotic systems.

Another way of obtaining the energy levels and stationary states has been pioneered by Gutzwiller [2]. It relies on a different approach. The Feynman path integral is a formulation of quantum mechanics equivalent to the Schrödinger equation. The amplitude of an elementary quantum process—going from point q to point q' in time t , i.e., the

matrix element $\langle q'|U(t)|q\rangle$ of the evolution operator—is expressed as a sum over all possible paths (classical as well as nonclassical ones) connecting the initial point to the final point, the phase being the classical action along the path divided by \hbar . In the semiclassical limit, the sum is computed using a stationary phase approximation. The action being stationary along *classical* paths, this results in the so-called Van Vleck semiclassical propagator, written here for simplicity for a one-dimensional system (extension to multidimensional systems is straightforward):

$$\langle q'|U(t)|q\rangle = \left(\frac{1}{2\pi i\hbar}\right)^{1/2} \sum_p \left|\frac{\partial^2 S_p(q,q',t)}{\partial q \partial q'}\right|^{1/2} \times \exp\left(\frac{iS_p(q,q',t)}{\hbar} - \frac{i\pi\nu_p}{2}\right), \quad (1)$$

where the index p labels all the classical trajectories going from q to q' in time t . The action S_p and the Maslov index ν_p are classical quantities.

This semiclassical propagator can be converted from the time domain to the energy domain with a second stationary phase approximation, leading to the semiclassical Green function of the system. The latter can be used to compute the density of states (this involves a third stationary phase approximation). For system with “hard chaos” (only isolated unstable periodic orbits), the final result is the so-called Gutzwiller trace formula [written here for two-dimensional (2D) systems]:

$$d(E) = \bar{d}(E) + \text{Im} \left[\sum_p \frac{T_p}{\pi\hbar \sqrt{\det(M_p - 1)}} \times \exp\left(\frac{iS_p}{\hbar} - \frac{i\nu_p\pi}{2}\right) \right]. \quad (2)$$

The first term $\bar{d}(E)$ is a smooth function (Thomas-Fermi approximation), and the second term is a sum over periodic

orbits having action S_p , period T_p , Maslov index ν_p , and where M_p denotes the classical stability matrix of the periodic orbit (also called monodromy matrix). Importantly, similar expressions can be obtained for integrable systems where periodic orbits are not isolated [1]. There, it can be shown to be *equivalent* to the EBK quantization method.

During the last few years, considerable effort has been devoted to the study of periodic orbit expansions pioneered by Gutzwiller [3–5]. The goal is to be able to compute the approximate positions of the quantum energy levels from the classical periodic orbits. This is in practice very hard to do, because of the sum over all classical periodic orbits whose number increases exponentially as a function of the period for classically chaotic systems.

To overcome the difficulties of periodic orbit expansions, a simple idea is to come back to the propagator in the time domain and use it to propagate *wave packets*. Various methods have been used for regular or chaotic systems [6–13]. The simplest idea—the so-called linear wave-packet dynamics—is to expand the semiclassical propagator in the vicinity of the wave-packet center and use such an expansion for propagating the quantum wave packet (for a review, see [11]). The difficulty is that, at long times, the initially localized wave packet spreads in phase space—very rapidly when the classical dynamics is chaotic—and any localization is consequently lost at long times. In other words, any local expansion in the vicinity of the wave-packet center can only be valid for a relatively short time. To overcome such a problem, “multiple trajectories” methods [8–10,14–17] have been studied. The most efficient one—called nonlinear wave-packet dynamics—has been developed by Heller and co-workers [14–17]. In the past few years, it has been successfully used in several systems, regular and chaotic: it is possible to reproduce the quantum interferences and spectra without any explicit quantization, looking at the classical evolution in phase space.

Section II of this paper describes the nonlinear wave-packet dynamics. In Sec. III, we show how the method can be used to describe any time-independent one-dimensional system, resulting in a universal behavior, among which are the well-known quantum collapse and quantum revival phenomena [18]. We demonstrate its explicit connection with the standard WKB method in Sec. IV. Finally, in Sec. V, we use these results to study the behavior of a hydrogen atom in a low magnetic field. This is a first step towards a semiclassical description of this system in a strong magnetic field, when the classical dynamics is chaotic.

II. NONLINEAR WAVE-PACKET DYNAMICS

We here describe the nonlinear wave-packet dynamics. The method relies on the fact that the wave-packet is initially small compared to the phase space volume. Indeed, the phase space volume of a wave packet—as it can be intuitively seen through the Wigner quasi-probability density $P_w(q,p,t)$ [19]—is of the order of \hbar^N , where N is the number of degrees of freedom. Therefore, the wave packet can be time-propagated using a local approximation of the Van Vleck propagator (or, equivalently, by a local expansion of the time-dependent Schrödinger equation). The simplest approach, worked out by Heller [6,7] and Littlejohn [11], uses

an expansion in the vicinity of the center of the wave packet. Although it is true that the center evolves according to the classical equations of motion, the wave-packet spreading limits the relevance of this approach to short times. To go further, one has to realize that the distortion of the wave packet is also mainly governed by classical equations. In classical mechanics, the initially localized wave packet develops more and more intricate structures in phase space as time goes on. So does the quantum wave packet: as time increases, the evolution of the wave packet cannot be described by a single distorted wave packet, but different local approximations (depending on which part of the wave packet one is interested in) have to be used. This is the key point of the “nonlinear wave-packet dynamics” [14–17].

In order to illustrate the principle of the method, let us consider an interesting quantum quantity: the overlap between the time propagated and the initial wave packets (autocorrelation function). If $\psi(q,t)$ denotes the wave packet, the autocorrelation function is written as

$$C(t) = \langle \psi(0) | \psi(t) \rangle = \int \psi^*(q,t=0) \psi(q,t) dq. \quad (3)$$

It gives an idea of how different a wave packet is from its initial shape. It is also a quantity which can be experimentally measured, see recent experiments using atomic wave packets excited with short pulsed lasers [20–22]. The autocorrelation function is simply related to the eigenstates and energy levels of the system through the equation [obtained by expanding the propagator $U(t) = \exp(-iHt/\hbar)$ on the eigenstates]

$$C(t) = \langle \psi(0) | U(t) | \psi(0) \rangle = \sum_K |\langle \psi(t=0) | \phi_K \rangle|^2 e^{-iE_K t/\hbar}. \quad (4)$$

$|\phi_K\rangle$ and E_K are the eigenstates and energy levels of the system. In Eq. (4), one sees that the quantized states can interfere destructively (collapses) or constructively (revivals) [18], depending on the various energy levels and eigenstates.

In order to estimate a semiclassical approximation of the autocorrelation function, we use the semiclassical Van Vleck propagator, Eq. (1), in Eq. (3), which gives

$$C(t) = \int \psi^*(q,0) \left\{ \left(\frac{1}{2\pi i \hbar} \right)^{1/2} \int \sum_p \left| \frac{\partial^2 S_p(q',q,t)}{\partial q \partial q'} \right|^{1/2} \times \exp \left(i \frac{S_p(q',q,t)}{\hbar} - i \frac{\pi \nu_p}{2} \right) \psi(q',0) dq' \right\} dq, \quad (5)$$

where p labels all the classical trajectories which link q' to q during the time t . As $\psi(q)$ is important only in a limited region of space, the trajectories starting from various initial points q and ending at various points q' having similar shapes can be *grouped* together. The total contribution of a given family of orbits can be estimated using a local expansion to the classical quantities entering in Eq. (5). This local expansion has to be done in the vicinity of a “reference” trajectory j roughly situated at the “center” of the family of trajectories. The quantity inside the braces in Eq. (5), when estimated by such a local approximation, represents a local

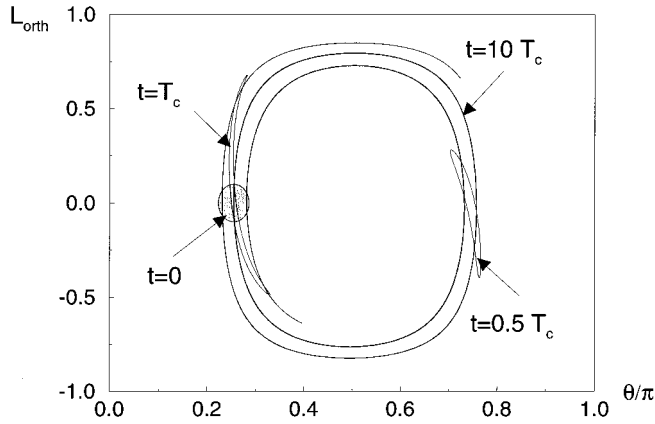


FIG. 1. Distortion with time of the phase-space region where the Wigner function of the initial localized wave packet takes its maximum values. It is drawn here for a hydrogen atom in a weak magnetic field, a problem which is effectively a one-dimensional problem when described in the canonical variables (L_{\perp}, θ) (see Sec. V). At $t=0$, since the wave packet is Gaussian, this surface is an ellipsis (shaded). T_c is the classical period of the motion of the center of the initial wave packet (most probable location at $t=0$). The initial wave packet is propagated according to the classical equations of motion, and distorts since each point is the initial condition of a different probable trajectory of the particle. After a time $0.5T_c$, there is no overlap between the initial and propagated surfaces: the autocorrelation function $C(t) = \int \psi^*(q, t=0) \psi(q, t) dq$ is (at this degree of approximation) equal to 0. After $t=T_c$, there is one intersection between the propagated and initial wave packets: to evaluate the autocorrelation function, only the distortion of the wave packet in the vicinity of the central trajectory is needed. But for $t=10T_c$, there are three distinct intersections between the initial and propagated wave packets: the distortions of the initial wave packet along those three reference trajectories are needed to calculate the autocorrelation function, Eq. (42).

approximation $\psi_j(q, t)$ of the initial wave packet propagated during time t . This is an “elementary” wave-packet solution of the Schrödinger equation expanded in the vicinity of the classical reference trajectory j . It is important to note that the expansion is *not* made around the wave-packet center, but around a classical trajectory relevant for the part of the propagated wave packet one wants to describe.

The total autocorrelation function is obtained as a sum (thus including interference terms) over the various j contributions:

$$C(t) = \sum_j \int \psi^*(q, t=0) \psi_j(q, t) dq. \quad (6)$$

Classical mechanics tells us how to choose the reference trajectories. This is illustrated in Fig. 1, in the case of the hydrogen atom in a weak magnetic field. It is a one-dimensional problem (see Sec. V), and the projection of a localized wave packet in phase space (its Wigner distribution) is then a surface. In Fig. 1, we show the initial wave packet (shaded), represented by an ellipsis in the case of a Gaussian wave packet, and the time propagated wave packets in phase space. We have plotted the distortion of the initial wave packet through the classical equations of motion,

each point of the surface having a different initial condition. T_c is the classical period of the motion of the center of the initial wave packet. After time $0.5T_c$, there is no overlap between the initial and propagated surfaces: no reference trajectory is found and the autocorrelation is consequently equal to 0 (within the degree of approximation we use; of course, the exact autocorrelation is not strictly 0, but vanishingly small). After one classical period ($t=T_c$), there is one intersection between the initial and propagated surfaces, at the center of which we choose the reference trajectory: only one reference trajectory will contribute to the autocorrelation function, and the linear wave-packets dynamics still holds. But after ten classical periods ($t=10T_c$), there are three distinct intersections and three different reference trajectories are needed to evaluate the autocorrelation function, Eq. (6).

The great advantage of looking at the projection of the wave packet in phase space through the Wigner transform is to be able to select the proper sets j of classical trajectories, and to replace the propagation along all the trajectories of one set by the propagation of the wave packet in the vicinity of one reference trajectory for each set j . This method also shows clearly the link between classical and quantum mechanics: since the particle is represented by a volume in the quantum phase space (it is a point in the classical phase space), there are several intersections j possible, and then interferences.

III. ONE-DIMENSIONAL TIME INDEPENDENT SYSTEM

In this section, we use the nonlinear wave-packet dynamics to study a general one-dimensional time independent system, for which the classical Hamiltonian will be written $H(q, p)$. We here bring together results and techniques already worked out in the context of wave-packet dynamics and show how they can be used for the nonlinear wave-packet dynamics. In Sec. III A, we recall the basic formula for the autocorrelation function already derived by Heller and co-workers [17]. In Secs. III B and III C, we study the propagation of an elementary wave packet along a *single* reference trajectory, using the techniques worked out for the linear wave-packet dynamics [6,11]. In Sec. III D, following the work of Littlejohn [11,12], we show that for a general Hamiltonian [not necessarily of the form $H = p^2/2 + V(q)$], the use of action-angle coordinates leads to substantially simpler results. The final formula—to be used in the following sections—is obtained in Sec. III E. Although none of the ingredients used is fully original, it is the first time to our knowledge that they are put together in the framework of *multiple trajectories* (nonlinear) wave-packet dynamics in a comprehensive study.

A. Calculation of the autocorrelation function

The conservation of energy gives one constant of motion: since the system is 1D and time independent, it is integrable. It is now experimentally possible to excite very localized wave packets [20–25]. Quantally, the coherent sum of eigenstates is such that the probability density is peaked with minimum fluctuations (minimum phase space size of \hbar): this is a Gaussian wave packet. Besides, we know that a Gaussian wave packet does not spread in a harmonic potential, and that the quantum averages for such a wave packet are the

classical ones. We will then start from such a wave packet, initially at position q_c with momentum p_c , whose wave function is (we use $\hbar=1$ throughout the rest of this paper)

$$\psi(q, t=0) = (\pi\sigma_0^2)^{-1/4} \exp\left\{ip_c(q-q_c) - \frac{(q-q_c)^2}{2\sigma_0^2}\right\}. \quad (7)$$

The width σ_0 is an arbitrary parameter which we can choose freely. The Wigner transform [19] of such a wave packet gives its density quasiprobability in phase space:

$$P_w(p, q) = \exp\left\{-\sigma_0^2(p-p_c)^2 - \frac{(q-q_c)^2}{\sigma_0^2}\right\}. \quad (8)$$

It is obviously Gaussian in p and q and has an ‘‘area’’ equal to 1, the value of the Planck constant in our units. One can imagine it as a set of initial conditions, and thus of possible trajectories with a Gaussian weight.

As explained in Sec. II, in order to semiclassically estimate the autocorrelation function, we have to look at the distortion of the wave packet along reference trajectories which are closed after time t , and which are localized in phase-space regions where the initial wave packet takes large values. A second order expansion of the Hamiltonian in the vicinity of the reference trajectory leads to a propagated wave packet $\psi_j(q, t)$ which is still a Gaussian wave packet written as

$$\begin{aligned} \psi_j(q, t) = & (\pi\sigma_0^2)^{-1/4} \exp\{i\{\xi_j(t)[q-q_j(t)] \\ & + \alpha_j(t)[q-q_j(t)]^2 + \gamma_j(t)\}. \end{aligned} \quad (9)$$

When the wave packet evolves with time, the functions $\xi_j(t)$, $\alpha_j(t)$, and $\gamma_j(t)$ express the distortion of the wave packet whose center travels along the classical trajectory $(q_j(t), p_j(t))$. Their initial conditions are easily derived from Eq. (7):

$$\begin{aligned} \xi_j(0) &= p_c + \frac{i[q_j(0) - q_c]}{\sigma_0^2}, \\ \alpha_j(0) &= \frac{i}{2\sigma_0^2}, \\ \gamma_j(0) &= [q_j(0) - q_c] \left(p_c + \frac{i[q_j(0) - q_c]}{2\sigma_0^2} \right). \end{aligned} \quad (10)$$

The autocorrelation function can then be rewritten as a sum (over all the reference trajectories) of the overlaps between the initial wave packet and the elementary propagated wave packets $\psi_j(q, t)$ [17]:

$$\begin{aligned} C(t) = & \sum_j \left(\frac{2\alpha_j(0)}{\alpha_j(t) - \alpha_j^*(0)} \right)^{1/2} \exp\left\{i\left(\gamma_j(t) - \gamma_j^*(0) \right. \right. \\ & \left. \left. - \frac{[\xi_j(t) - \xi_j^*(0)]^2}{4[\alpha_j(t) - \alpha_j^*(0)]}\right)\right\}. \end{aligned} \quad (11)$$

In the following, we determine the quantities α, ξ, γ relative to each elementary propagated wave packet $\psi_j(q, t)$. For

each elementary wave packet, the procedure is equivalent to monotrajjectory (linear) wave-packet dynamics, which has been widely studied [6,11].

B. Evolution of the wave packet along a reference trajectory

In this section, we derive the equations of propagation for an elementary wave packet evolving along the reference trajectory j . From the preceding section, we know that quantumly the wave packet will evolve along the trajectory j with the Schrödinger equation:

$$i \frac{\partial \psi_j(q, t)}{\partial t} = \hat{H}_j(\hat{q}, \hat{p}, t) \psi_j(q, t), \quad (12)$$

where (\hat{p}, \hat{q}) denote quantum operators:

$$\hat{p} = \frac{\hbar}{i} \frac{\partial}{\partial q}. \quad (13)$$

$\hat{H}_j(\hat{q}, \hat{p}, t)$ is the quantum Hamiltonian of the particle expanded to second order around $(q_j(t), p_j(t))$, to account for the local behavior of the wave function in the vicinity of the reference trajectory j .

Using Hamilton’s equations for classical motion, we obtain for the quantum Hamiltonian

$$\begin{aligned} \hat{H}_j(\hat{q}, \hat{p}, t) = & H(q_j(t), p_j(t)) + \dot{q}_j(t)[\hat{p} - p_j(t)] \\ & - \dot{p}_j(t)[\hat{q} - q_j(t)] + \frac{K_{11}(j, t)}{2} [\hat{q} - q_j(t)]^2 \\ & + \frac{K_{12}(j, t)}{2} [\hat{q} - q_j(t)][\hat{p} - p_j(t)] + \frac{K_{21}(j, t)}{2} \\ & \times [\hat{p} - p_j(t)][\hat{q} - q_j(t)] + \frac{K_{22}(j, t)}{2} [\hat{p} - p_j(t)]^2, \end{aligned} \quad (14)$$

where the dot denotes the derivative of a classical quantity with respect to t and $K_{lm}(j, t)$ matrix contains the second derivatives of the Hamiltonian with respect to q, p along the trajectory j (see below). It is a purely classical quantity, contrary to \hat{q} and \hat{p} which are quantum operators. Besides, the conservation of energy implies $H(q_j(t), p_j(t)) = H(q_j(0), p_j(0)) = E_j$. Note, however, that E_j is *not* the central energy of the wave packet, it is just the energy of the reference trajectory.

$\hat{H}_j(\hat{q}, \hat{p}, t)$ is then an operator quadratic in $-i\hbar\partial/\partial q$ and \hat{q} . Plugging Eqs. (14) and (9) in Eq. (12), one obtains coupled ordinary differential equations for the functions $\xi_j(t), \alpha_j(t)$, and $\gamma_j(t)$, which we call ‘‘distortion’’ equations as they describe the distortion of an elementary wave packet:

$$\dot{\xi}_j = \dot{p}_j - \left[2K_{22}\alpha_j + \frac{(K_{12} + K_{21})}{2} \right] (\xi_j - p_j), \quad (15)$$

$$\dot{\alpha}_j = -\frac{K_{11}}{2} - (K_{12} + K_{21})\alpha_j - 2K_{22}\alpha_j^2, \quad (16)$$

$$\dot{\gamma}_j = -E_j + \dot{q}_j p_j - \frac{K_{22}}{2} (\xi_j - p_j)^2 + i \left(K_{22} \alpha_j + \frac{K_{12}}{2} \right), \quad (17)$$

where $p_j = p_j(t)$ and $q_j = q_j(t)$ are solutions of the classical equations of motion for the trajectory j . Remember that the K matrix is time dependent.

C. Solutions of the distortion equations along a reference trajectory

We first solve the differential equation for α_j , Eq. (16). In this section, we drop the index j , since the equations are similar for all the trajectories j . All the derivatives are taken along the reference trajectory $(q(t), p(t)) = (q_j(t), p_j(t))$.

Let us consider a classical trajectory $(q'(t), p'(t))$ neighboring the trajectory $(q(t), p(t))$, and denote

$$\begin{aligned} \delta q(t) &= q'(t) - q(t), \\ \delta p(t) &= p'(t) - p(t), \end{aligned} \quad (18)$$

the deviations from the reference trajectory. According to Hamilton's equations, a small initial deviation $(\delta q(0), \delta p(0))$ is related to the deviation at time t by the monodromy matrix:

$$\begin{pmatrix} \delta q(t) \\ \delta p(t) \end{pmatrix} = \begin{pmatrix} \frac{\partial q(t)}{\partial q(0)} & \frac{\partial q(t)}{\partial p(0)} \\ \frac{\partial p(t)}{\partial q(0)} & \frac{\partial p(t)}{\partial p(0)} \end{pmatrix} \begin{pmatrix} \delta q(0) \\ \delta p(0) \end{pmatrix}. \quad (19)$$

This matrix will be denoted $M(t)$. It obeys the following equation of evolution:

$$\frac{dM(t)}{dt} = JK(t)M(t), \quad (20)$$

with

$$K(t) = \begin{pmatrix} \frac{\partial^2 H}{\partial q^2} & \frac{\partial^2 H}{\partial q \partial p} \\ \frac{\partial^2 H}{\partial p \partial q} & \frac{\partial^2 H}{\partial p^2} \end{pmatrix} \quad (21)$$

and

$$J = \begin{pmatrix} 0 & 1 \\ -1 & 0 \end{pmatrix}. \quad (22)$$

A straightforward calculation shows that, whatever the initial conditions $(\delta q(0), \delta p(0))$, the quantity [17]

$$\alpha(t) = \frac{1}{2} \frac{\delta p(t)}{\delta q(t)} = \frac{1}{2} \left(\frac{M_{21}(t) \delta q(0) + M_{22}(t) \delta p(0)}{M_{11}(t) \delta q(0) + M_{12}(t) \delta p(0)} \right) \quad (23)$$

is a solution of Eq. (16) [26]. Among the family of solutions, we are interested in the one satisfying the initial condition, Eq. (10). We obtain the solution $\alpha(t)$ as a function of the monodromy matrix:

$$\alpha(t) = \frac{1}{2} \left(\frac{M_{21}(t) \sigma_0^2 + i M_{22}(t)}{M_{11}(t) \sigma_0^2 + i M_{12}(t)} \right). \quad (24)$$

Knowing $\alpha(t)$, we can proceed solving Eqs. (17) and (15). From Eq. (20), we deduce

$$\begin{aligned} \frac{\delta \dot{q}(t)}{\delta q(t)} &= K_{21}(t) + K_{22}(t) \frac{\delta p(t)}{\delta q(t)} \\ &= K_{21}(t) + K_{22}(t) 2\alpha(t). \end{aligned} \quad (25)$$

Since $K_{12}(t) = K_{21}(t)$, Eq. (15) can be written

$$\frac{\dot{\xi}(t) - \dot{p}(t)}{\xi(t) - p(t)} = - \frac{\delta \dot{q}(t)}{\delta q(t)}, \quad (26)$$

the general solution of which is

$$\begin{aligned} \xi(t) - p(t) &= \frac{[\xi(0) - p(0)] \delta q(0)}{M_{11}(t) \delta q(0) + M_{12}(t) \delta p(0)} \\ &= \frac{\xi(0) - p(0)}{M_{11}(t) + 2\alpha(0) M_{12}(t)}. \end{aligned} \quad (27)$$

For the specific initial conditions in Eq. (10), we obtain the desired solution

$$\xi(t) - p(t) = \frac{\sigma_0^2 [p_c - p(0)] + i [q(0) - q_c]}{M_{11}(t) \sigma_0^2 + i M_{12}(t)}. \quad (28)$$

Finally, we have all the elements needed to solve Eq. (17). Using Eqs. (25) and (27), this equation can be rewritten

$$\begin{aligned} \dot{\gamma}(t) &= -E + p \dot{q} - \frac{K_{22}(t)}{2} \left(\frac{[\xi(0) - p(0)] \delta q(0)}{M_{11}(t) \delta q(0) + M_{12}(t) \delta p(0)} \right)^2 \\ &\quad + \frac{i}{2} \frac{\delta \dot{q}(t)}{\delta q(t)}. \end{aligned} \quad (29)$$

Its general solution is obtained by elementary quadratures:

$$\begin{aligned} \gamma(t) &= -Et + \int p dq - \frac{[\xi(0) - p(0)]^2 M_{12}(t) \delta q(0)}{2 [M_{11}(t) \delta q(0) + M_{12}(t) \delta p(0)]} \\ &\quad + \frac{i}{2} \ln \left\{ \frac{M_{11}(t) \delta q(0) + M_{12}(t) \delta p(0)}{\delta q(0)} \right\} + \gamma(0). \end{aligned} \quad (30)$$

The desired solution, satisfying the initial condition Eq. (10), is thus

$$\begin{aligned} \gamma(t) &= -Et + \int p dq \\ &\quad - \frac{\{\sigma_0^2 [p_c - p(0)] + i [q(0) - q_c]\}^2 M_{12}(t)}{2 \sigma_0^2 [\sigma_0^2 M_{11}(t) + i M_{12}(t)]} \\ &\quad + \frac{i}{2} \ln \left\{ M_{11}(t) + \frac{i}{\sigma_0^2} M_{12}(t) \right\} + \gamma(0). \end{aligned} \quad (31)$$

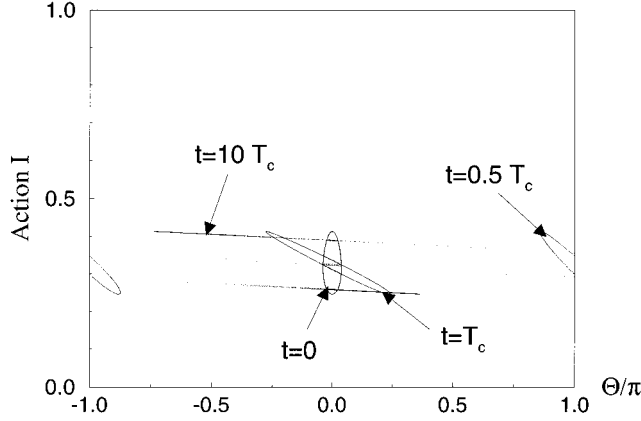


FIG. 2. Same as Fig. 1 plotted now in action-angle coordinates (I, Θ) . The initial wave packet is also an ellipsis in the (I, Θ) phase space (shaded). The classical propagation is extremely simple: the action I is constant while Θ increases linearly with time, at a rate depending on I . Again, after $t=0.5T_c$, the initial and propagated wave packets have no overlap. There are three distinct intersections after $t=10T_c$, which implies that three reference trajectories are needed to calculate the autocorrelation function, Eq. (42).

From the previous solutions, Eqs. (24), (28), and (31) of the distortion equations, we can obtain the semiclassical expression for the autocorrelation function, Eq. (11).

D. Action-angle variables

In the (q, p) variables, the monodromy matrix does not have a simple expression. Following the original idea of Littlejohn [11,13], we show in this section that action-angle variables lead to simpler expressions.

Since we are dealing with a 1D time independent, and thus integrable system, there are action-angle variables (I, Θ) , such that [2]

$$2\pi I = \oint_{\text{period}} p dq, \quad (32)$$

$$\{I, \Theta\} = 1. \quad (33)$$

The first advantage of the action-angle variables is that the determination of the reference trajectories is extremely simple. Figure 2 shows the analog of Fig. 1, the distortion of the initial wave packet as times goes on, but in action-angle coordinates. The global motion is then along curves with fixed action I at a velocity in Θ which is constant in time, but depending on I . The reference closed trajectories just correspond to an increase of the angle Θ by an integer multiple of 2π during time t . Thus, the reference trajectories can be labeled by a single integer j corresponding to an increase of Θ by $2\pi j$. An immediate consequence is that the reference trajectory j is the j th repetition of a primitive periodic orbit. In the initial (q, p) coordinates, j counts the number of loops done in time t along the primitive periodic orbit, see Fig. 1.

Each reference orbit can be characterized by its action I_j , the corresponding period of the primitive orbit being

$$T_j = \frac{2\pi}{\left. \frac{\partial H}{\partial I} \right|_{I_j}}. \quad (34)$$

The condition defining the reference orbit j is simply

$$T_j = \frac{t}{j} \quad (35)$$

or

$$\left. \frac{\partial H}{\partial I} \right|_{I_j} = \frac{2\pi j}{t}. \quad (36)$$

A second advantage of the action-angle variables is that, since I is constant, and $H = H(I)$, the monodromy matrix is very simple. Indeed, from Eq. (21), all the elements of matrix K are equal to 0, except $K_{22} = \partial^2 H / \partial I^2$. Hence, the monodromy matrix $\mathcal{M}(t)$ in action-angle coordinates is [13]

$$\mathcal{M} = \begin{pmatrix} 1 & \frac{\partial^2 H}{\partial I^2} t \\ 0 & 1 \end{pmatrix}. \quad (37)$$

If $P(t)$ is the transfer matrix between the two sets of coordinates (of determinant 1 as both are canonical sets of coordinates), we deduce (we are in the vicinity of a classical trajectory which is closed after time t) the monodromy matrix in the initial coordinates, for each reference trajectory:

$$M(t) = \begin{pmatrix} 1 + P_{21} P_{22} \frac{\partial^2 H}{\partial I^2} t & P_{22}^2 \frac{\partial^2 H}{\partial I^2} t \\ -P_{21}^2 \frac{\partial^2 H}{\partial I^2} t & 1 - P_{21} P_{22} \frac{\partial^2 H}{\partial I^2} t \end{pmatrix}, \quad (38)$$

where $P_{lm} = P_{lm}(0)$ and $\partial^2 H / \partial I^2$ are constants only determined by the initial position $(q(0), p(0))$.

Here, all the elements of the monodromy matrix are linear (plus constant) functions of time t , which makes the evolutions of $\alpha(t)$, $\xi(t)$, and $\gamma(t)$, hence of the autocorrelation function, very simple. Note that these simple relations hold only because closed reference trajectories are used. When t is not a multiple integer of the period, the elements of the monodromy matrix are no longer linear functions of time.

E. Final expression of the autocorrelation function

The expressions can be further simplified if one chooses as initial starting point for launching the wave packet a turning point of the classical motion such that $\dot{q}(0) = 0$, that is $P_{22} = 0$ (note, however, that this is not a serious limitation and quite simple expressions can also be obtained if the wave packet is launched anywhere). The monodromy matrix then reduces to

$$M(t) = \begin{pmatrix} 1 & 0 \\ -P_{21}^2 \frac{\partial^2 H}{\partial I^2} t & 1 \end{pmatrix}. \quad (39)$$

The solutions of the distortion equations are the following simple expressions:

$$\begin{aligned} \xi(t) &= \xi(0), \\ \alpha(t) &= \alpha(0) - \frac{1}{2} P_{21}(0)^2 \frac{\partial^2 H}{\partial I^2} t, \end{aligned} \quad (40)$$

$$\gamma(t) = -Et + I \frac{\partial H}{\partial I} t + \gamma(0) - \nu \frac{\pi}{2},$$

where the classical quantity $P_{21}(0) = (\partial I / \partial q)_{(q(0), p(0))}$ as well as the action and related quantities can be derived from the Hamiltonian and equations of motion in (q, p) . The constant term $\nu\pi/2$ comes from the logarithmic term in Eq. (31). Indeed, the argument of the logarithm $M_{11}(t) + iM_{12}(t)/\sigma_0^2$ has the same value at the ending and starting points of the reference trajectory. However, along the trajectory, its logarithm has to evolve continuously. Depending on the “trajectory” of the quantity $M_{11}(t) + iM_{12}(t)/\sigma_0^2$ in complex plane, the determination of the logarithm at the ending point may differ from its original value by $i\nu\pi$, with ν an even integer which is the Maslov index of the trajectory. It is also the number of turning points (caustics) along the trajectory. For a reference orbit j which is the j th repetition of a primitive orbit, the Maslov index is simply j times the one of the primitive orbit. This term, as emphasized by Heller and co-workers [7,9,10], is a “smooth Maslov index,” continuously accumulated along one trajectory, to be added in the phase of their semiclassical wave functions. Using the concepts of symplectic and metaplectic operators, Littlejohn derived its expression [13], noticing that with the wave-packets methods, the phase shift is not due to turning points, in contrast with the usual WKB picture where the Maslov index comes from the failure of the semiclassical approximation at the turning points. Thus here also, and contrary to the WKB approach, there is in general no breakdown of our *phase space* semiclassical approximation near turning points [27].

In the following, we write for a reference trajectory j

$$A_j = P_{21}(0)^2 \left(\frac{\partial^2 H}{\partial I^2} \right)_{I_j} = \left(\frac{\partial I}{\partial q} \right)_{q_j(0)}^2 \left(\frac{\partial^2 H}{\partial I^2} \right)_{I_j}. \quad (41)$$

We are now able to evaluate all the elements of $C(t)$ in Eq. (11), using Eqs. (10), (40), and (41). We obtain the following expression for the autocorrelation function:

$$C(t) = \sum_j \left(1 + i \frac{\sigma_0^2}{2} A_j t \right)^{-1/2} \exp \left\{ - \frac{i[q_j(0) - q_c]^2 A_j t}{2 \left(1 + i \frac{\sigma_0^2}{2} A_j t \right)} - iH(I_j)t + i2\pi j \left(I_j - \frac{\nu_j}{4} \right) \right\}, \quad (42)$$

where the sum over the index j involves all the reference orbits making j loops along a primitive periodic orbit during time t . The equation defining the reference orbit j is Eq. (36), with the initial (and final) conditions $(q_j(0), \dot{q}_j(0) = 0)$. The Maslov index ν_j in Eq. (42) is the one of the primitive orbit. Typically, all the primitive reference orbits have similar shapes and equal Maslov indices.

Equation (42) is the final expression for the semiclassical autocorrelation function. It is one important result of this paper, as it is valid for any one-dimensional time independent system. Its simplicity lies in the fact that as soon as the $H(I)$ function—the energy as a function of the action—is known, all the ingredients are easily computed.

IV. COMPARISON WITH WKB QUANTIZATION

In the preceding Sec. III, we computed the autocorrelation function of an initially localized wave packet using the distortion of a surface in phase space, whose points follow the classical equations of motion. No quantization has been introduced. Before turning to application to a specific system (the hydrogen atom in a weak magnetic field), we discuss in this section the link between our semiclassical approach using time propagation and the standard “stationary” WKB approach.

Related work has been done in the framework of *monotrajectory* (linear) wave-packet dynamics. De Leon and Heller [10] showed that at first order around the central trajectory, the WKB spectrum is obtained using a monotrajectory method. Once more, the difficulty comes from the spreading of the wave packet, which limits the validity of the method to the short time domain and consequently the accuracy of the computed energy levels. Littlejohn [12] also derived the WKB spectrum from a monotrajectory wave-packet propagation, introducing a fictitious parameter of evolution (different from the usual time).

Finally, it was numerically shown in the specific case of the hydrogen atom [17], that the Fourier transform of the autocorrelation function obtained by the nonlinear wave-packet dynamics has peaks located at the position of the quantum (or WKB, as they coincide in the very special case studied) levels.

In this section, we completely solve this problem for the *multiple trajectories* (nonlinear) wave-packet dynamics. We first show that if we keep the full set of reference trajectories, but expand their properties (action, period, . . .) around the central orbit of the wave packet at second order, we obtain for the autocorrelation function Eq. (42), a result which is strictly equivalent to the corresponding *second order* approximation in the WKB method. Of course, this approximation breaks down at very long times. There, we analytically

show that the Fourier transform of the autocorrelation function has δ peaks lying *exactly* at the positions of the WKB energy levels.

A. Expansion of the reference orbits in the vicinity of the central orbit

If the initial wave packet is well localized in phase space (a basic assumption in the nonlinear wave-packet dynamics), all the reference orbits having an important weight start (and end) in a small range of initial conditions around the center of the wave packet. Thus, all these reference trajectories have roughly similar actions and periods. In other words, at any time t , the number Δj of reference orbits significantly contributing to the autocorrelation function, Eq. (42), is much smaller than j itself. Hence, we can use local approximations of the various classical quantities involved in Eq. (42). These local approximations are obtained by expansions in the vicinity of the central orbit, defined as the classical orbit followed by the initial center of the wave packet (q_c, p_c) . At arbitrary time t , this central orbit is of course not closed. We define j_c , the noninteger value equal to the number of loops performed along the central orbit in time t :

$$j_c = \frac{t}{T_c} = \frac{t}{2\pi} \frac{\partial H}{\partial I} \Big|_{I_c}, \quad (43)$$

where I_c, T_c are the action and period of the central orbit.

We now consistently expand the classical quantities referring to the reference orbit j in Eq. (42) around j_c at second order in powers of $j - j_c$. Note that such an expansion is required for the last terms in the exponential, because they rapidly oscillate with j , but not for the prefactor and the first term of the exponential which are very smooth functions.

A straightforward calculation gives the following expression of the autocorrelation function:

$$C(t) = \frac{e^{-iH(I_c)t}}{\sqrt{1 + i \frac{\Sigma^2}{2} \left(\frac{\partial^2 H}{\partial I^2} \right)_{I_c} t}} \sum_j \exp \left\{ 2i\pi j \left(I_c - \frac{\nu_c}{4} \right) - \frac{\pi^2 \Sigma^2 (j - j_c)^2}{1 + i \frac{\Sigma^2}{2} \left(\frac{\partial^2 H}{\partial I^2} \right)_{I_c} t} \right\}, \quad (44)$$

where we define

$$\Sigma^2 = \sigma_0^2 \left(\frac{\partial I}{\partial q} \right)_{q_c}^2. \quad (45)$$

This sum over integer values j can be transformed using the Poisson sum formula [18] to another sum over the integer K :

$$C(t) = \frac{1}{\sqrt{\pi \Sigma^2}} \sum_K \exp \left(- \frac{\left(K + \frac{\nu_c}{4} - I_c \right)^2}{\Sigma^2} \right) \times \exp \left\{ -i \left[H(I_c) + \left(\frac{\partial H}{\partial I} \right)_{I_c} \left(K + \frac{\nu_c}{4} - I_c \right) + \frac{1}{2} \left(\frac{\partial^2 H}{\partial I^2} \right)_{I_c} \left(K + \frac{\nu_c}{4} - I_c \right)^2 \right] t \right\}. \quad (46)$$

Consistently at second order, the term in the second exponential is nothing but the classical Hamiltonian H evaluated at the action $K + \nu_c/4$:

$$C(t) = \sum_K \frac{\exp \left\{ - \frac{\left(K + \nu_c/4 - I_c \right)^2}{\Sigma^2} \right\}}{\sqrt{\pi \Sigma^2}} e^{-iE_K t}. \quad (47)$$

A comparison with Eq. (4) shows that this is exactly a quantum autocorrelation function, with energy levels given by

$$E_K = H \left(I = K + \frac{\nu_c}{4} \right). \quad (48)$$

These energy levels are the classical energies where the action, Eq. (32), is equal to

$$\oint_{\text{period}} p dq = 2\pi \left(K + \frac{\nu_c}{4} \right), \quad K \text{ integer}. \quad (49)$$

For the simplest case $\nu_c = 2$, the action is equal to a half integer multiple of 2π . This is exactly the result of the WKB quantization. Moreover, Eq. (47) shows that the coefficients of the expansion of the initial wave packet onto the eigenstates have a Gaussian distribution centered on the central energy of the wave packet:

$$\left| \int \psi^*(q, 0) \phi_K(q) dq \right|^2 = \frac{1}{\sqrt{\pi \Sigma^2}} \exp \left\{ - \frac{\left(K + \nu_c/4 - I_c \right)^2}{\Sigma^2} \right\}. \quad (50)$$

This proves that, at second order around the center of the wave packet, the nonlinear wave-packet dynamics is exactly equivalent to the usual WKB approximation.

Equation (44) has additional consequences. Indeed, the obtained autocorrelation function depends only on 3 independent parameters. The first two, $I_c - \nu_c/4$ and $\partial^2 H / \partial I^2$, are related to the period of the classical motion and to its dispersive character, while the third, Σ^2 , just specifies the extension of the wave packet. Equation (44) thus contains the well known behavior of a one-dimensional wave packet [18]. At short time, only one (or zero) reference trajectory significantly contributes. Thus the autocorrelation function oscillates periodically at the frequency of the classical motion. After some time—depending on the dispersive character of the dynamics and on Σ^2 —the wave packet broadens and the autocorrelation function decreases [this is the role of the prefactor in Eq. (44)]. At longer time, several reference tra-

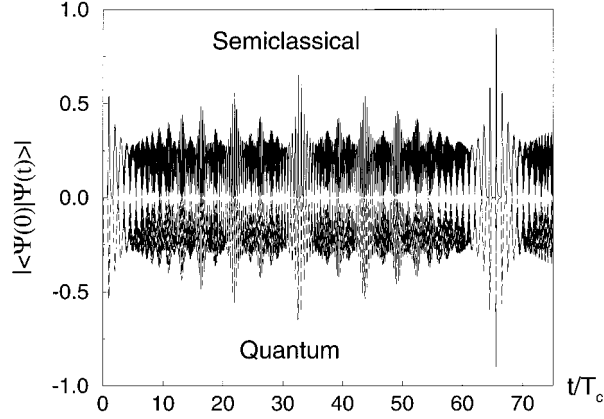


FIG. 3. Modulus of the autocorrelation function for an initially Gaussian wave packet of the hydrogen atom in a weak magnetic field. The wave packets considered here are purely angular wave packets, obtained by linear combinations of the low-field diamagnetic states with fixed value of the magnetic quantum number $m=0$ and fixed value of the principal quantum number $n_0=100$ (first order perturbation theory). Hence, the classical dynamics of the system is effectively one-dimensional (see Fig. 1). The autocorrelation function is the overlap between the initial and the time propagated wave packets $\langle\psi(0)|\psi(t)\rangle$. The unit of time is the classical period of the central trajectory T_c (trajectory of the center of the initial wave packet). Above (solid line), the result obtained by the nonlinear wave packet dynamics, Eq. (42) and below, represented as a mirror image (long-dashed line), the result of the quantum calculation in the same perturbative conditions. The collapse ($t \approx 5T_c$), fractional revivals ($t \approx 22T_c$ for the one third, $t \approx 33T_c$ for the half revival), and revivals ($t \approx 65T_c$ for the first one) of the wave packet, are perfectly semiclassically reproduced, by taking into account the distortion of the wave packet in the vicinity of the classical trajectories closed at each time t .

jectories interfere, leading to a collapse of the wave packet. Finally, at long time, the different j contributions may come back in phase, leading to the so-called revival of the wave packet [18]. An example of such a behavior is given in Fig. 3 and is discussed in Sec. V on a specific system. Equation (44) proves that this behavior is universal among the one-dimensional time independent systems.

At extremely long time, the second order expansion must fail as the higher order corrections are multiplied by the time t in Eq. (42) and can thus become arbitrarily large. There, the nonlinear wave-packet dynamics differs from the WKB approximation. As shown in Sec. V, the nonlinear wave-packet dynamics gives a much better approximation to the exact quantum result. The reason is not fully understood.

It is possible to get more insight into the compared properties of the two semiclassical methods by computing the Fourier transform of the autocorrelation function:

$$C(E) = \frac{1}{2\pi} \int_{-\infty}^{+\infty} C(t) \exp(iEt) dt. \quad (51)$$

If $C(t)$ is the exact quantum autocorrelation function, then $C(E)$ displays δ peaks at the positions of the quantum energy levels. If $C(t)$ is the WKB autocorrelation function, then $C(E)$ also displays δ peaks but at the positions of the

WKB energy levels. Nothing of that type can be proved for the semiclassical $C(t)$, Eq. (42). However, for its approximation at second order, Eq. (44), it is true that the Fourier transform is discrete, which is already an important result. Indeed, we started from an approximate expression for the time propagator. As the (purely quantum) discreteness of the energy spectrum implies delicate phase relations in the propagator, it is unexpected that the approximations made preserve this discreteness. It is an indication that nonlinear wave-packet dynamics is even better than naively thought.

Although we are not able to calculate exactly $C(E)$ using the semiclassical $C(t)$, Eq. (42), we can locate its main singularities. Indeed, substitution of $C(t)$ by its semiclassical expression gives

$$\frac{1}{2\pi} \sum_j \int_{-\infty}^{+\infty} \left(1 + i \frac{\sigma_0^2}{2} A_j t\right)^{-1/2} \exp\left\{-\frac{i[q_j(0) - q_c]^2 A_j t}{2 \left(1 + i \frac{\sigma_0^2}{2} A_j t\right)} + i[E - H(I_j)]t + i2\pi j \left(I_j - \frac{\nu_j}{4}\right)\right\} dt. \quad (52)$$

In this formula, we will perform the integral over t at fixed j , and subsequently sum the various j contributions.

As the integral over t runs between $-\infty$ and $+\infty$, it is asymptotically dominated by longtime, i.e., large j contributions [see Eq. (34)]. For such large j , the last two terms in the exponential are rapidly changing. We can thus evaluate the integral over t by the stationary phase approximation. The phase of the integrand is

$$\varphi_j(E, t) = [E - H(I_j)]t + 2\pi j \left(I_j - \frac{\nu_j}{4}\right). \quad (53)$$

Its derivative with respect to t is simply evaluated [taking into account that I_j depends on t through Eq. (36)]:

$$\frac{\partial \varphi_j(E, t)}{\partial t} = E - H(I_j). \quad (54)$$

Thus, the phase is stationary when the reference trajectory has precisely the energy E . It is not surprising that only trajectories with precisely energy E significantly contribute to the Fourier spectrum at energy E . Note that this trajectory is the same for all the j values. Its action, denoted I_E , is such that $H(I_E) = E$.

The second derivative of the phase φ_j at the extremum point $E = H(I_E)$ is

$$\left(\frac{\partial^2 \varphi_j(E, t)}{\partial t^2}\right)_{H(I_E)=E} = \frac{4\pi^2 j^2}{t^3} \frac{1}{\left(\frac{\partial^2 H}{\partial I^2}\right)_{I_E}} \quad (55)$$

which gives

$$C(E) = \frac{\sqrt{\left(\frac{\partial^2 H}{\partial I^2}\right)_{I_E}}}{\sqrt{2\pi} \left|\left(\frac{\partial H}{\partial I}\right)_{I_E}\right|} \sum_j \frac{e^{i\pi/4} t^{1/2}}{\left(1 + i \frac{\sigma_0^2}{2} A_j t\right)^{1/2}} \times \exp\left\{-\frac{i(q_E - q_c)^2 A_E t}{2\left(1 + i \frac{\sigma_0^2}{2} A_E t\right)}\right\} \exp\left[2i\pi j \left(I_E - \frac{\nu_E}{4}\right)\right], \quad (56)$$

where A_E, I_E, q_E , and ν_E characterize the trajectory with energy E .

t and j are related by

$$\left(\frac{\partial H}{\partial I}\right)_{I_E} = \frac{2\pi j}{t}. \quad (57)$$

The sum over j in Eq. (56) is asymptotically dominated by the large j values, for which the $i(\sigma_0^2/2)A_E t$ term is much larger than 1. This gives the asymptotic contribution to $C(E)$, using Eq. (41):

$$C(E) = \frac{1}{\left|\left(\frac{\partial H}{\partial I}\right)_{I_E}\right|} \frac{1}{\sqrt{\pi\sigma_0^2 \left(\frac{\partial I}{\partial q}\right)_{q_E}^2}} \times \exp\left\{-\frac{(q_E - q_c)^2}{\sigma_0^2}\right\} \sum_j \exp\left[2i\pi j \left(I_E - \frac{\nu_E}{4}\right)\right]. \quad (58)$$

The latter sum is nothing but a sum of δ peaks:

$$C(E) = \frac{1}{\left|\left(\frac{\partial H}{\partial I}\right)_{I_E}\right|} \frac{1}{\sqrt{\pi\sigma_0^2 \left(\frac{\partial I}{\partial q}\right)_{q_E}^2}} \times \exp\left\{-\frac{(q_E - q_c)^2}{\sigma_0^2}\right\} \sum_K \delta\left(I_E - \frac{\nu_E}{4} - K\right), \quad (59)$$

where K is an integer.

This can be again rewritten as

$$C(E) = \frac{1}{\sqrt{\pi\sigma_0^2 \left(\frac{\partial I}{\partial q}\right)_{q_E}^2}} \exp\left\{-\frac{(q_E - q_c)^2}{\sigma_0^2}\right\} \sum_K \delta(E - E_K), \quad (60)$$

where E_K are the WKB energy levels such that

$$E_K = H\left(I = K + \frac{\nu}{4}\right). \quad (61)$$

Thus the Fourier spectrum of the autocorrelation function has δ peaks located *exactly* at the positions of the WKB energy levels. At the second order, ones also rediscovers the

Gaussian distribution of amplitudes of the wave packet on the eigenstates, Eqs. (47) and (50).

As mentioned above, Eq. (60) is not the exact Fourier spectrum of the semiclassical autocorrelation function, but only its leading singularities. Additional ‘‘background’’ especially coming from small j contributions exist. As shown in Sec. V, a simple numerical experiment proves that the leading singularities are dominant by far.

Thus, we can conclude that in the energy domain, the nonlinear wave-packets dynamics is strictly equivalent to the WKB method, as it gives exactly the same discrete spectrum. In the time domain, it is not clear *a priori* which method is the best. Numerical experiments in Sec. V show that the nonlinear wave-packets dynamics gives more accurate results.

V. AN EXAMPLE: THE HYDROGEN ATOM IN A WEAK MAGNETIC FIELD

A. The hydrogen atom in a magnetic field

Neglecting spin, relativistic, QED, effects, the Hamiltonian of a hydrogen atom in a uniform magnetic field along the Oz axis is, in atomic units [28,29],

$$H = \frac{p^2}{2} - \frac{1}{r} - \frac{\gamma}{2} L_z + \frac{\gamma^2}{8} (x^2 + y^2), \quad (62)$$

where $\gamma = B/B_c$ and $B_c = 2.35 \times 10^5$ T is the atomic unit of magnetic field. L_z , the z component of the angular momentum, is a constant. In the following, we consider only the case $L_z = m = 0$.

The classical dynamics of the system depends on the scaled energy $\epsilon = E\gamma^{-2/3}$ [29]. At low magnetic field ($\epsilon \ll -1$), it is quasi-integrable; around $\epsilon = -0.5$, a significant part of the phase space turns chaotic; almost full chaos is reached around $\epsilon = -0.13$. The quantum energy spectrum evolves in accordance with a change in the statistical properties of the energy levels [29,30].

When the magnetic field is sufficiently weak, the diamagnetic term $V = \gamma^2(x^2 + y^2)/8$ can be considered as a perturbation. Quantally, this means that the degeneracy ($0 \leq l \leq n-1$) of the Rydberg levels is removed, and that each level of principal quantum number n is split in n sub-levels labeled by the new quantum number K ranging from 0 to $n-1$ [35]. The energy levels E_{nmK} and the associated diamagnetic eigenstates $|nmK\rangle$ are obtained by diagonalization of the perturbation inside a manifold n . This is the so-called ‘‘ l -mixing’’ regime [31–33]. The diamagnetic eigenstates are linear combinations of the usual spherical $|nlm\rangle$ states for $0 \leq l \leq n-1$ with field independent coefficients. Alternatively, they can be expanded in the so-called ‘‘parabolic’’ basis [31].

In the following, we study exclusively this low-field perturbative regime, where n and m are good quantum numbers. The wave packets to be considered are linear combinations of $|nmK\rangle$ eigenstates. As there is only one relevant quantum number K , this is an effectively one-dimensional problem. The wave packets are thus purely angular ones along the spherical θ coordinate, being completely delocalized along the radial coordinate and the azimuthal angle. The quantum calculations described in this section are obtained by the

straightforward formula, Eq. (4), where $|\phi_K\rangle = |nmK\rangle$ are the diamagnetic states, whose energies are

$$E_K = -\frac{1}{2n^2} + \frac{\gamma^2}{8} \langle nmK | x^2 + y^2 | nmK \rangle. \quad (63)$$

In classical mechanics, the analog of the quantum first order perturbation theory is the secular (or adiabatic) approximation [31]: the effect of the magnetic field is so weak that the motion can be described as an instantaneous field-free motion, that is a Kepler elliptical trajectory of the electron around the nucleus. The weak magnetic field induces a slow secular motion of the parameters (orientation, major axis, eccentricity) of the elliptical trajectory. The secular motion is described by an effective Hamiltonian, which is nothing but the value of the diamagnetic perturbation averaged over an unperturbed elliptical trajectory. The result is simply expressed as a function of the constants of motion on an elliptical trajectory: the angular momentum \vec{L} and the Runge-Lenz vector \vec{A} (along the major axis of the ellipsis with modulus equal to its eccentricity):

$$\vec{L} = \vec{r} \times \vec{p}, \quad (64)$$

$$\vec{A} = \vec{p} \times \vec{L} - \frac{\vec{r}}{r}. \quad (65)$$

The expression for the effective secular Hamiltonian is

$$\mathcal{H} = \left\langle \gamma^2 \frac{x^2 + y^2}{8} \right\rangle = \frac{\gamma^2}{64E_0^2} (\Lambda + 1), \quad (66)$$

where E_0 is the (constant) unperturbed energy and

$$\Lambda = 4\vec{A}^2 - 5A_z^2. \quad (67)$$

For the case we are interested in, $L_z = 0$, the secular motion can be simply described by a set of two canonically conjugate coordinates: θ the angle between the z axis and the Runge-Lenz vector \vec{A} , and L_\perp the component of the angular momentum perpendicular to the plane defined by the unit vector \vec{u}_z along z and \vec{A} [32]:

$$\theta = \angle(\vec{u}_z, \vec{A}), \quad (68)$$

$$L_\perp = \vec{L} \cdot \frac{\vec{u}_z \times \vec{A}}{\|\vec{u}_z \times \vec{A}\|}.$$

The Poisson bracket is the canonical one:

$$\{L_\perp, \theta\} = 1. \quad (69)$$

The original three-dimensional problem is thus reduced—using the constancy of L_z and the secular approximation—to a one-dimensional problem whose phase-space variables are $(q, p) = (\theta, L_\perp)$. In these coordinates, the effective Hamiltonian, Eq. (66), is

$$\Lambda(\theta, L_\perp) = (5 \sin^2 \theta - 1)(1 + 2E_0 L_\perp^2). \quad (70)$$

The equations of motion are obtained using the usual Hamilton's equation:

$$\frac{d\theta}{dt} = \{\mathcal{H}, \theta\} = \frac{\gamma^2}{16E_0} [5 \sin^2(\theta) - 1] L_\perp, \quad (71)$$

$$\frac{dL_\perp}{dt} = \{\mathcal{H}, L_\perp\} = -\frac{\gamma^2}{64E_0^2} 5 \sin(2\theta)(1 + 2E_0 L_\perp^2).$$

This one-dimensional Hamiltonian system can be solved by elementary quadratures. There are two possible types of motion, depending on the sign of the constant Λ . The separatrix between the two types of motion is $\Lambda = 0$ or, equivalently is associated with a critical value of the angle θ [31,32]

$$\theta_{cr} = \arcsin\left(\sqrt{\frac{1}{5}}\right) \approx 0.4636. \quad (72)$$

For $\theta_0 \leq \theta_{cr}$ or $\theta_0 \geq \pi - \theta_{cr}$ ($-1 \leq \Lambda \leq 0$), the secular motion is an oscillation of the Runge-Lenz vector around the Oz axis, and is called vibrational. For $\pi - \theta_{cr} \geq \theta_0 \geq \theta_{cr}$ ($0 \leq \Lambda \leq 4$), the secular motion is an oscillation of the Runge-Lenz vector around the $z=0$ plane, and is called rotational. Equation (70) shows that θ oscillates between 0 and θ_{max} (or $\pi - \theta_{max}$ and π) for the vibrational motion, and θ_{max} and $\pi - \theta_{max}$ for the rotational motion, with

$$\theta_{max} = \arcsin\left(\sqrt{\frac{\Lambda + 1}{5}}\right).$$

B. Analytical results for the secular motion

We now compute all the quantities needed for the semiclassical propagation of wave packets and calculation of the autocorrelation function, Eq. (42). For all these quantities—action-angle coordinates, energy and its first two derivatives with respect to the action, monodromy matrix, and Maslov index—we are able to obtain analytic results as functions of elliptic integrals. In the following, we consider a trajectory as a solution of Eq. (71). It is characterized by a set of initial conditions $(\theta(0), L_\perp(0))$.

The first quantity to compute is the action variable along a trajectory $I = \oint L_\perp d\theta / 2\pi$ as a function of the energy, which implicitly determines the function $\mathcal{H}(I)$ needed in Eq. (42). The result is easily expressed as a function of Λ and involves elliptic integrals of the first and third kind [36]

$$K(r) = \int_0^{\pi/2} \frac{d\phi}{\sqrt{1-r \sin^2(\phi)}}, \quad (73)$$

$$\Pi(p, r) = \int_0^{\pi/2} \frac{d\phi}{[1-p \sin^2(\phi)] \sqrt{1-r \sin^2(\phi)}}. \quad (74)$$

We obtain

$$I_v(\Lambda) = -\frac{\Lambda}{\pi} \sqrt{\frac{1}{-2E_0(4-\Lambda)}} \left[\Pi\left(1+\Lambda, \frac{4(1+\Lambda)}{4-\Lambda}\right) - K\left(\frac{4(1+\Lambda)}{4-\Lambda}\right) \right] (\text{vibrational}), \quad (75)$$

$$I_r(\Lambda) = \frac{\Lambda}{\pi} \sqrt{\frac{1}{-2E_0(1+\Lambda)}} \left[\Pi\left(\frac{4-\Lambda}{4}, \frac{4-\Lambda}{4(1+\Lambda)}\right) - K\left(\frac{4-\Lambda}{4(1+\Lambda)}\right) \right] (\text{rotational}). \quad (76)$$

The period of the motion then follows directly from Eq. (34):

$$T_v(\Lambda) = \frac{16(-2E_0)^{3/2}}{\gamma^2 \sqrt{4-\Lambda}} K\left(\frac{4(1+\Lambda)}{4-\Lambda}\right) (\text{vibrational}), \quad (77)$$

$$T_r(\Lambda) = -\frac{16(-2E_0)^{3/2}}{\gamma^2 \sqrt{1+\Lambda}} K\left(\frac{4-\Lambda}{4(1+\Lambda)}\right) (\text{rotational}). \quad (78)$$

Note that for the rotational motion, the energy \mathcal{H} , i.e., Λ , decreases with the action I_r . The rotational period is thus negative. This simply means that negative values of the integer j have to be included in the sum, Eq. (42).

The next term needed to calculate the autocorrelation function is the quantity A_j , Eq. (41), which can be rewritten as

$$A = -\frac{25\gamma^2 \sin^2 2\theta(0)}{64E_0^2} \frac{\partial T}{T(\Lambda)}, \quad (79)$$

which holds for both vibrational and rotational cases, with the respective form for the periods. Equations (77) and (78) give [denoting: $K'(r) = dK/dr$]

$$\frac{\partial T_v}{\partial \Lambda} = \frac{\gamma^2}{32(-2E_0)^{3/2}} \frac{T_v(\Lambda)^2}{K\left(\frac{4(1+\Lambda)}{4-\Lambda}\right)^2 \sqrt{4-\Lambda}} \times \left[K\left(\frac{4(1+\Lambda)}{4-\Lambda}\right) + 40 \frac{K'\left(\frac{4(1+\Lambda)}{4-\Lambda}\right)}{4-\Lambda} \right], \quad (80)$$

$$\frac{\partial T_r}{\partial \Lambda} = \frac{\gamma^2}{32(-2E_0)^{3/2}} \frac{T_r(\Lambda)^2}{K\left(\frac{4-\Lambda}{4(1+\Lambda)}\right)^2 \sqrt{1+\Lambda}} \times \left[K\left(\frac{4-\Lambda}{4(1+\Lambda)}\right) + \frac{5}{2} \frac{K'\left(\frac{4-\Lambda}{4(1+\Lambda)}\right)}{1+\Lambda} \right]. \quad (81)$$

The last classical quantity needed is the Maslov index. For all rotational trajectories (the ones studied hereafter), there are just two turning points at θ_{max} and $\pi - \theta_{max}$ and thus $\nu = 2$.

C. Semiclassical calculations

We have applied the nonlinear wave-packet dynamics to an initial wave packet:

$$\psi(\theta, t=0) = (\pi\sigma_0^2)^{-1/4} \exp\left\{-\frac{(\theta-\theta_c)^2}{2\sigma_0^2}\right\}. \quad (82)$$

Indeed, as explained in Sec. III, in order to simplify the calculations, for a given trajectory (central or reference), we start from a Kepler ellipse making an angle $\theta(0)$ with the Oz axis, in an extremal position $\theta_{max} = \theta(0)$, which here implies in addition $L_\perp = 0$.

Then, to evaluate the autocorrelation function Eq. (42) at time t , we determine all the values of Λ such that [see Eq. (35)]

$$t = jT(\Lambda_j) \quad (83)$$

in a certain interval imposed by the width σ_0 of the Gaussian. In all the calculations and figures presented hereafter, the necessary truncation of the sum in j is such that the error on the autocorrelation function is negligible.

When these reference trajectories are determined, the equations derived in Sec. V B allow us to calculate the autocorrelation function Eq. (42) for a state of energy E_0 of the hydrogen atom perturbed by a weak uniform magnetic field.

D. Quantum calculations

All the results presented in this section concern the hydrogen atom in a weak uniform magnetic field. In this case, the quantal equivalent of the state, Eq. (82), is an extremal eigenstate of energy $E_0 = -1/2n_0^2$ of the hydrogen atom without magnetic field, having the maximum value $(n_0 - 1)$ of the Runge-Lenz vector \vec{A} along the direction making an angle θ_c with the Oz axis.

We have calculated that it is indeed a wave packet whose distribution on the quantum eigenstates of energy E_K obtained by diagonalization of the diamagnetic perturbation, Eq. (66) inside the manifold of energy E_0 is approximately

$$|\langle \psi(0) | \phi_K \rangle| \propto \exp\left(-\frac{(\theta_K - \theta_c)^2}{2\sigma_0^2}\right) \quad (84)$$

with

$$\sigma_0^2 = \frac{1}{n_0}. \quad (85)$$

We then have an exact quantum calculation with which to compare our semiclassical results.

In all the figures, the initial state is chosen such that $\theta_c = 0.8$ (corresponding to a rotational motion) and $n_0 = 100$. As we are using first order perturbation theory, the magnetic field strength is unimportant. Indeed, if one uses the classical period of the central orbit as unit of time, the

autocorrelation function is independent of γ . The energy spectrum itself is of course γ dependent. We used $\gamma = 10^{-7}$ a.u., that is roughly 0.0235 T.

E. The autocorrelation function

In all the figures shown, the solid line is the autocorrelation function obtained from the nonlinear wave-packet dynamics, Eq. (42), the long-dashed line is the exact quantum result, and the dotted line is the autocorrelation function obtained by WKB semiclassical quantization [WKB energy levels in Eq. (4), and initial Gaussian distribution].

Figure 3 shows the comparison, over more than 70 classical periods of the motion, between the moduli $|C(t)|$ of the semiclassical and quantum autocorrelation functions. We see that, although no quantization has been introduced in the nonlinear wave-packets dynamics, which deals only with classical trajectories, the quantum autocorrelation function is almost perfectly reproduced. At short time, the autocorrelation function comes back close to its initial maximum value 1 at integer multiples of the classical period. This corresponds to a still localized wave packet following the classical evolution. There, only one reference orbit significantly contributes to the semiclassical autocorrelation function, resulting in a simple analytic form. However, the successive maxima are lower and lower, indicating a dispersion (collapse) of the wave packet [18]. In Eq. (42), this corresponds to the slowly decreasing prefactor of the exponential. Around $t = 4T_c$, the wave packet has sufficiently spread for its head to interfere with the tail. The autocorrelation function then looks very complicated. It results from the interferences between several reference trajectories.

At a longer time, around $t = 65T_c$, $C(t)$ is again very large, almost reaching 1. This is the quantum ‘‘revival’’ of the wave packet [18]. In the quantum autocorrelation function, Eq. (4), it appears as a local rephasing of the contributions of the various eigenstates. In the semiclassical picture, Eq. (42), it appears as a constructive interference between all the reference trajectories. From Eq. (44), we deduce the expression of the revival time:

$$T_{\text{revival}} = \frac{2\pi}{\left(\frac{\partial^2 H}{\partial I^2}\right)_{I_c}}, \quad (86)$$

which is in excellent agreement with the observation in Fig. 3. At intermediate times, one can see ‘‘fractional revivals’’ [18] where only a subset of the eigenstates (or a subset of the reference trajectories: they are related via the Poisson sum formula; see Sec. IV) interfere constructively.

In Fig. 4 we show that the agreement is not only global, but that the details of the quantum autocorrelation function are very accurately reproduced by the nonlinear wave-packet dynamics. They are better reproduced than using the WKB quantization.

In Fig. 5, we show the different autocorrelation functions at very short time, when only one or two reference trajectories are used to calculate the autocorrelation function. Even in this case, the nonlinear wave-packet dynamics result is much closer to the quantum result than the WKB result. Note that, instead of using the distribution Eq. (84) in Eq. (4), we

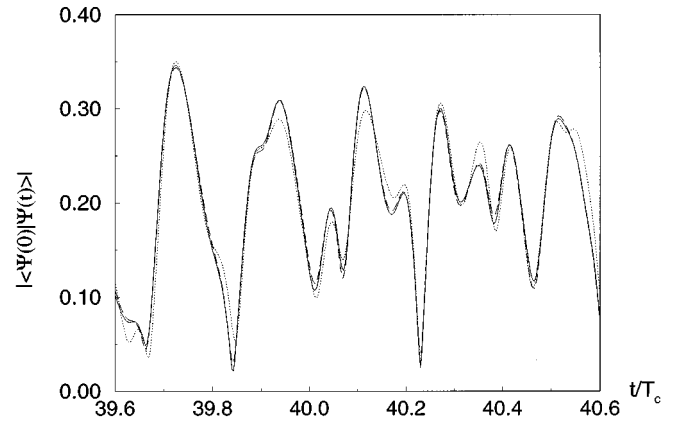


FIG. 4. Detail of Fig. 3: autocorrelation functions corresponding to the propagation of the same initial Gaussian wave packet (electron of the hydrogen atom in a weak uniform magnetic field) by three different methods: quantum (long-dashed), nonlinear wave-packet dynamics (solid line), and exact WKB semiclassical quantization (dotted line). The nonlinear wave-packet dynamics reproduces much more accurately the quantum behavior than the WKB quantization, although no explicit quantization has been introduced.

also used the exact quantum overlaps: the nonlinear wave-packets dynamics is still much better than the WKB quantization.

In Fig. 6, results are shown at extremely long time (almost 6000 classical periods). We then see that both nonlinear wave-packet dynamics and WKB results are a little out of phase from the quantum result, but that the nonlinear wave-packet dynamics reproduces very well the quantum shape when WKB can be very different.

Nonlinear wave-packet dynamics provides not only a better understanding of the semiclassical limit than WKB quantization, but is also much more accurate in the time domain. For very long times, it is the most efficient semiclassical method available.

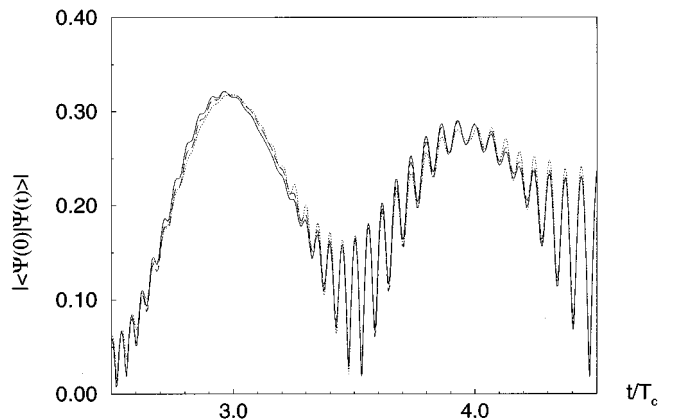


FIG. 5. Same as Fig. 4, but after few classical periods only, when the different parts of the initial wave packet have just spread sufficiently to interfere. The bumps at $t = 3$ and $t = 4$ represent the initial wave packet returning to its initial position after three and four classical periods, the fringes in between are due to interferences between the head and the tail of the wave packet. Once again, the nonlinear wave-packet dynamics reproduces more closely the quantum result than the WKB method.

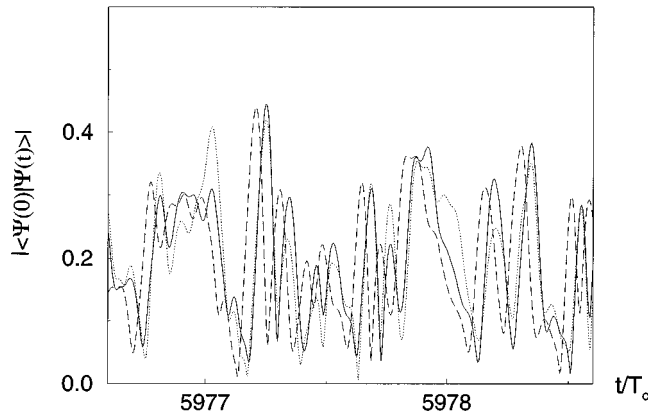


FIG. 6. Same as Fig. 4, but after a very long time: almost 6000 central classical periods T_c . The autocorrelation functions obtained by the quantum treatment (long-dashed) and the nonlinear wave-packet dynamics (solid line) have a very similar shape, except that they are slightly out of phase. The WKB result (dotted line) is similarly out of phase, but the shape of the autocorrelation function is much worse. This figure proves the outstanding efficiency of the nonlinear wave-packet dynamics, even at extremely long times.

F. Fourier spectra in the energy domain

Additional information on the nonlinear wave-packet dynamics can be obtained from the Fourier spectrum $C(E)$, Eq. (52). For the exact quantum autocorrelation function and when the Fourier transform is performed on an infinite time interval, it displays δ peaks at the positions of the energy levels. When the Fourier transform is performed on a finite range, the peaks are just broadened. The same is true for the WKB autocorrelation function, except that the peaks lie at the WKB energy levels. Starting from the semiclassical approximation of the autocorrelation function, Eq. (42), nothing ensures *a priori* that the Fourier spectrum will display discrete peaks.

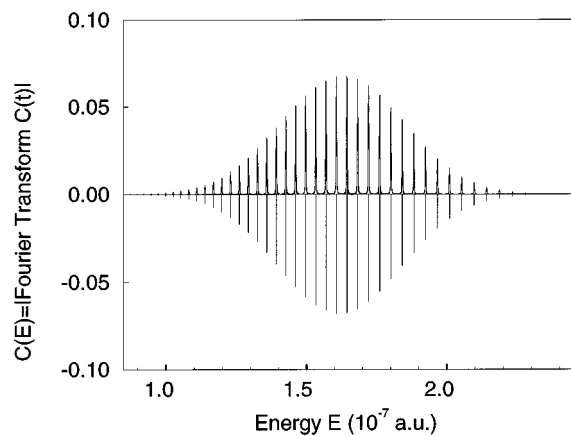


FIG. 7. Fourier transform of the autocorrelation function of Fig. 1, obtained semiclassically by the nonlinear wave-packet dynamics (time interval for the Fourier transform = 80 classical periods), compared to the quantum δ peaks, located at the energy levels E_K , and whose amplitude $|\langle \psi(0) | \phi_K \rangle|^2$ are the overlaps between the initial wave packet and the eigenstates $|\phi_K\rangle$ of the system. The *totality* of the quantum spectrum is perfectly reproduced by the semiclassical method.

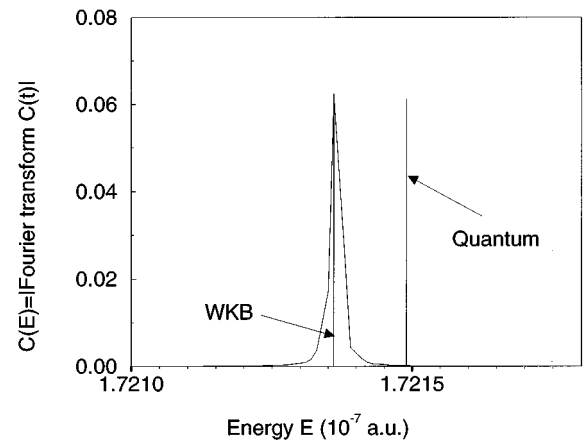


FIG. 8. Fourier transform of the semiclassical autocorrelation function performed over a very long time (≈ 2500 classical periods). What could not be seen in Fig. 7 is now visible: the levels obtained by Fourier transform of the semiclassical autocorrelation function, Eq. (42), are equal to the WKB energy levels, and not to the exact quantum levels. It is a remarkable property of the nonlinear wave-packet dynamics to give an autocorrelation function, Eq. (42), which has an almost discrete Fourier spectrum.

In Fig. 7, we show such a spectrum, compared to the exact quantum spectrum. The height of the quantum peaks is the overlap $|\langle \psi(0) | \phi_K \rangle|^2$ corresponding to the energy E_K , quantally calculated as explained above [see Eq. (4)]. The time interval is 80 classical periods, which is largely enough to resolve the individual energy levels. It is remarkable that, without any explicit quantization, the nonlinear wave-packet dynamics is able to reproduce the *totality* of the quantum

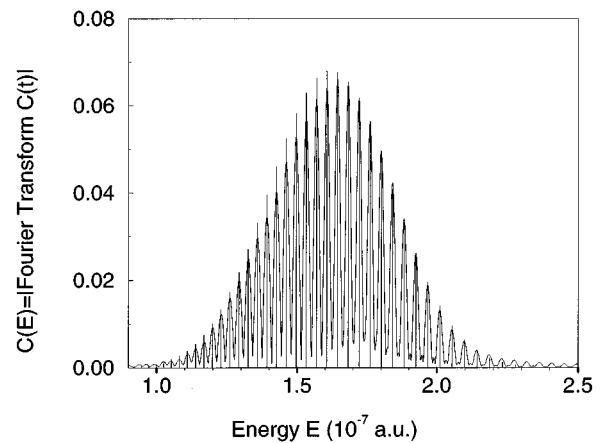


FIG. 9. Same as Fig. 7, but the Fourier transform is now performed over a very short time interval, ≈ 2.5 classical periods of the central trajectory of the initial wave packet (two first peaks of Fig. 3). Here, the spreading of the wave packet is such that the semiclassical autocorrelation function is computed using only *one* reference trajectory in Eq. (42). Nevertheless, the discrete character of the energy spectrum is already visible with a good accuracy. This proves that purely quantum properties can be obtained without interferences between different trajectories. In fact, the Fourier transform allows us to observe the interference between one primitive trajectory and its repetitions at longer times.

energy spectrum. This implies that the various approximations done to obtain Eq. (42)—semiclassical approximation for the Van Vleck propagator and grouping of the various classical trajectories in sets whose global effect is represented by a single reference trajectory—preserve almost exactly the discrete nature of the Fourier spectrum.

Figure 8 is analogous to Fig. 7, but with a far better resolution, since it has been performed over a time interval of 2500 classical periods. The peaks are much narrower (and still Fourier limited), which makes it possible to observe that they do not lie exactly at the positions of the quantum energy levels, but rather at the WKB energy levels in agreement with the discussion in Sec. IV. It is not yet clear why, in the time domain, the nonlinear wave-packets dynamics is much closer to the quantum result than the WKB result, while they give the same energy levels.

But even more striking is Fig. 9, where we show the Fourier transform of the semiclassical autocorrelation function over a very short interval of time (≈ 2.5 classical periods T_c of the central trajectory of the initial wave packet). There is only *one* single reference trajectory which contributes to

the autocorrelation function, Eq. (42). But we see that the individual energy levels are nevertheless resolved. This implies that, contrary to a commonly accepted statement, there is no need to have interferences between different classical trajectories to obtain a quantized discrete energy spectrum. We here have quantum mechanics without interferences. Of course, this is not exactly true: interferences are indeed present in Eq. (42), even when the sum over j is reduced to only one term. This is because different closed reference trajectories are involved, depending on the time t considered. It is in this respect very different from Ref. [10], where the WKB spectrum was obtained through a wave packet propagated around one trajectory fixed in advance. In fact, what happens here is that the same reference trajectory is involved at time t and at time $2t$. Then, through the Fourier transform, the interference between two identical trajectories at different times produces the pattern of energy levels. It is the analog of an optical multiple wave interferometer—such as a Fabry-Pérot interferometer—considered here in the time domain.

-
- [1] M.V. Berry, in *Semi-classical Mechanics of Regular and Irregular Motion*, Les Houches Summer School, Session XXXVI, *Chaotic Behavior of Deterministic Systems*, edited by Gerard Iooss, Robert H.G. Helleman, and Raymond Stora (North-Holland, Amsterdam, 1981).
- [2] M.C. Gutzwiller, *Chaos in Classical and Quantum Mechanics* (Springer-Verlag, New York, 1990).
- [3] P. Cvitanovic and B. Eckhardt, Phys. Rev. Lett. **63**, 823 (1989).
- [4] G. Tanner, P. Scherer, E.B. Bogolmony, B. Eckhardt, and D. Wintgen, Phys. Rev. Lett. **67**, 2410 (1991).
- [5] T. Szeredi and D.A. Goodings, Phys. Rev. Lett. **69**, 1640 (1992).
- [6] E.J. Heller, J. Chem. Phys. **62**, 1544 (1975).
- [7] E.J. Heller, J. Chem. Phys. **67**, 3339 (1977).
- [8] M.J. Davis and E.J. Heller, J. Chem. Phys. **75**, 3916 (1981).
- [9] N. De Leon and E.J. Heller, J. Chem. Phys. **78**, 4005 (1983).
- [10] N. De Leon and E.J. Heller, J. Chem. Phys. **81**, 5957 (1984).
- [11] R.G. Littlejohn, Phys. Rep. **138**, 193 (1986).
- [12] R.G. Littlejohn, Phys. Rev. Lett. **56**, 2000 (1986).
- [13] R.G. Littlejohn and J.M. Robbins, Phys. Rev. A **36**, 2953 (1987).
- [14] S. Tomsovic and E.J. Heller, Phys. Rev. Lett. **67**, 664 (1991); Phys. Rev. E **47**, 282 (1993); Phys. Rev. Lett. **70**, 1405 (1993).
- [15] P.W. O'Connor, S. Tomsovic, and E.J. Heller, Physica (Amsterdam) **55D**, 340 (1992).
- [16] M.A. Sepúlveda, S. Tomsovic, and E.J. Heller, Phys. Rev. Lett. **69**, 402 (1992).
- [17] I.M. Suarez Barnes, M. Nauenberg, M. Nockleby, and S. Tomsovic, Phys. Rev. Lett. **71**, 1961 (1993); J. Phys. A **27**, 3299 (1994).
- [18] M. Nauenberg, Phys. Rev. A **40**, 1133 (1989); J. Phys. B **23**, L385 (1990).
- [19] M. Hillery, R.F. O'Connell, M.O. Scully, and E.P. Wigner, Phys. Rep. **106**, 121 (1984).
- [20] J. Parker and C. R. Stroud, Jr., Phys. Rev. Lett. **56**, 716 (1986).
- [21] L. Marmet, H. Held, G. Raithel, J. A. Yeazell, and H. Walther, Phys. Rev. Lett. **72**, 3779 (1994).
- [22] J. Wals, H.H. Fielding, J.F. Christian, L.C. Snoek, W.J. van der Zande, and H.B. van Linden van den Heuvell, Phys. Rev. Lett. **72**, 3783 (1994).
- [23] M. Mallalieu and C.R. Stroud, Jr., Phys. Rev. A **51**, 1827 (1995).
- [24] J.A. Yeazell and C.R. Stroud, Jr., Phys. Rev. Lett. **60**, 1494 (1988).
- [25] J.A. Yeazell and C.R. Stroud, Jr., Phys. Rev. A **43**, 5153 (1991).
- [26] The reason for which $\alpha(t)$ can be written under the simple form (23) is easily understood from the classical propagation in phase space. Indeed, the ellipsis representing the initial wave packet (see Fig. 1) evolves according to the classical equations of motion linearized in the vicinity of the orbit of reference. Therefore, the evolution of its major and minor axis is described by the monodromy matrix. The local wave packet evolves in the same way, $\alpha(t)$ being related to the orientation of the ellipsis associated with the Wigner distribution $P_w(q,p,t)$: it has to be related to $(\delta q(t), \delta p(t))$, hence to the monodromy matrix. Note, however, that the orbit $(q'(t), p'(t))$ is in no way a "real" orbit, but rather an orbit living in a complexified phase space.
- [27] The one-dimensional hydrogen atom is a singular case for which this approximation breaks down at the collision between the electron and the Coulomb singularity. In fact, the nonlinear wave-packet dynamics method works also in this case [17]. It is possible to show it by regularizing the Coulomb singularity using the semiparabolic coordinates and introducing a fictitious "oscillator" time which maps the problem on a harmonic oscillator problem [K. Dupret and D. Delande (unpublished)], the only difference being an unusual Maslov index.

- [28] D. Delande, in *Chaos in Atomic Systems*, Les Houches Summer School, Session LIII, *Fundamental Systems in Quantum Optics*, edited by J. Dalibard, J.M. Raymond, J. Zinn-Justin (North-Holland, Amsterdam, 1990).
- [29] H. Friedrich and D. Wintgen, *Phys. Rep.* **183**, 37 (1989).
- [30] D. Delande and J.C. Gay, *Phys. Rev. Lett.* **57**, 2006 (1986).
- [31] J.C. Gay and D. Delande, *Comm. At. Mol. Phys.* **13**, 275 (1983), and references therein.
- [32] E.A. Solov'ev, *Pis'ma Zh. Éksp. Teor. Fiz.* **34**, 278 (1981) [*JETP Lett.* **34**, 265 (1981)]; **82**, 1762 (1982) [**55**, 1017 (1982)].
- [33] D.R. Herrick, *Phys. Rev. A* **26**, 323 (1982).
- [34] A.P. Kasantzev, V.L. Pokrovsky, and J. Bergou, *Phys. Rev. A* **28**, 3659 (1983).
- [35] P.A. Braun, *Pis'ma Zh. Éksp. Teor. Fiz.* **84**, 890 (1983) [*JETP Lett.* **57**, 492 (1983)].
- [36] *Handbook of Mathematical Functions*, edited by M. Abramowitz and I.A. Stegun (Dover Publications, New York, 1972).